



Journal Homepage: [-www.journalijar.com](http://www.journalijar.com)

INTERNATIONAL JOURNAL OF ADVANCED RESEARCH (IJAR)

Article DOI:10.21474/IJAR01/13952
DOI URL: <http://dx.doi.org/10.21474/IJAR01/13952>



RESEARCH ARTICLE

MODELING AND PREDICTING THE MONO RIVER OVERFLOW UPSTREAM OF THE NANGBETO DAM IN WEST AFRICA USING MULTIPLICATIVE DETERMINIST MODEL

Taofic Bacharou^{1,2}, Vincent Prodjinto¹ and Côme Agossa Linsoussi³

1. Laboratory of Energetics and Applied Mechanics, Polytechnic School of Abomey-Calavi, University of Abomey-Calavi, 01 BP 2009 Cotonou, Benin.
2. Laboratory of Applied Ecology, Faculty of Agronomic Sciences, University of Abomey-Calavi. BP 526 Cotonou, Benin.
3. Laboratory of Applied Hydrology, Polytechnic School of Abomey-Calavi, 01 BP: 526 INE/UAC, Cotonou, Benin.

Manuscript Info

Manuscript History

Received: 20 October 2021

Final Accepted: 24 November 2021

Published: December 2021

Key words:-

Modeling, Nangbeto Dam, Flooding; Forecast, Deterministic Model, Mono River

Abstract

The variation and non-control of the overflow of the Mono River adversely affects the performance of the Nangbetohydropower plant to the point that it can no longer meet the increasingly increased demand for electricity. This study presents the development of an operational model for forecasting daily river flows for the plant's water retention. The overflow of the Mono River at the upstream hydroelectric dam from 1991 to 2019 was analyzed and modeled by the deterministic process with R software in order to make predictions. First, the flow series was analyzed by the ARIMA model (18, 1, 2) then by a multiplicative model after removing the seasonal trends from these series by the moving average method. The calculated error of the results of said model reveals that the deterministic model integrates the input generation processes with an error of the order of ($er = 28.26\%$). Finally, an annual flow forecasting program has been developed as a planning tool for the operation of the dam, in order to meet production needs and to plan water releases.

Copy Right, IJAR, 2021,. All rights reserved.

Introduction:-

Today, the evolution of technology allows the development of many forecasting tools in several fields such as hydrology [1], meteorology [2], economics [4], water treatment [5], etc. Hydrological forecasting models are not only very important for safety, especially in watersheds with hydroelectric installations with high water retention potential, but also allow an adequate and rapid response in crisis [6-7].

The energy from the hydroelectric dam, is very important for the economic development of modern societies [8]. The countries of Benin and Togo chose this option and in 1987 built the Nangbetohydroelectric dam on the Mono river through the Electricity Community of Benin (ECB) in order to induce a lasting economic impact on the energy supply [9]. However, the construction of large hydroelectric dams on water courses leads to changes in the hydrological and sedimentological regime that can lead to changes in the balance of the environment and have negative impacts on the life of the populations and the local economy [10- 11]. The example of the Aswan dam in Egypt is particularly striking in this regard [12]. Thus, the typical case of the Nangbeto dam, erected on the Mono

Corresponding Author:- Vincent Prodjinto

Address:- Laboratory of Energetics and Applied Mechanics, Polytechnic School of Abomey-Calavi, University of Abomey-Calavi, 01 BP 2009 Cotonou, Benin.

river since 1987, drastically modifies the natural hydro-sedimentary regime in the valley and at the mouth [13]. The Mono River drains a well-defined basin of about 30,000 km² and empties into the Atlantic Ocean through a vast system of lagoons [14]. Each year, unexpected floods, often caused by dramatic water releases, are observed in local communities with limited budgets already affected by cyclical floods [15-16]. The degradation and lack of climate control have favored in several regions of the world deadly floods following dams that have collapsed and, in some cases, have caused the reduction of the integrity of their structure.

To date, many researchers have already researched the dam deformation data prediction algorithm, and many conventional and efficient prediction algorithms have been developed. The most widely used model is the Autoregressive Integrated Moving Average (ARIMA) model. The ARIMA algorithm is an algorithm proposed by Box and other authors in the last century [1]. The existing literature systematically describes the ARIMA model, the AR model and the MA model, and establishes that the ARIMA model can well predict trends in time series. So it is used in various fields to predict time series data and get interesting results. For example, G. Xu et al used the ARIMA model to predict an original time series of dam deformation while Wang Wei and Jiancang Xie used the ARIMA model to predict monitoring data from the Lijia-xia reservoir [34]. Likewise, Genmiao Ye and Mengqian Huang applied the ARIMA model to a hydropower plant. The model is shown to have clear advantages for fitting and forecasting dam monitoring data. However, because the model cannot accurately reflect nonlinear characteristics between variables, as the prediction period increases, the accuracy of the prediction gradually decreases. A precise estimate of the available water and a good forecast of the daily intake are therefore essential to efficiently ensure the production of electrical energy. It will also help to minimize water loss and damage from discharges. It is therefore important to establish a model describing the supply flows of the dam and a program allowing the forecast.

Description Of The Study Area

The Nangbeto Dam is built in the Mono watershed, located in the Gulf of Guinea region. The Mono River rises in the northwest of Benin in the Koura Mountains of Bassila region. About 560 kilometers long, it serves as a natural border between Togo and Benin over its last 100 kilometers. Its watershed covers an area of 27,870 km² between latitudes 6°16' and 9°20' North and longitudes 0°42' and 2°45' East [20], so that it is inscribed in a rectangle oriented North-South, with a length of 340 km and a width of 118 km. The slightly uneven relief consists of coastal plains, plateaus, lagoons, and shallows. The vegetation is made up of dense semi-deciduous forests, riparian forests, gallery forests, savannahs, fallows, fields of crops, marsh meadows, and mangroves [9, 15, 21, 22]. Several ethnic groups made up mainly of farmers and fishermen live in the watershed [23]. The population density varies between 70 and 300 inhabitants / km².

Materials and Methods:-

Data Collection

The monthly hydrological data cover a period of 25 years (Table 1). In total, three hydrometric stations were taken into account (Figure 1). Note that the Nangbeto flow measurement station was unique before the construction of the dam (1955-1987). Since then, measurements have been made upstream and downstream of the dam (1988-1999).

Table 1:- Summary of data and characteristics of stations.

Types of data	Sources	Area or Station	Period	Characteristics		
				Latitude	Longitude	Altitude (m)
Water flows	CEB	Upstream Nangbéto	1991-2019	7°25'N	1°26'E	150
	CEB	Nangbéto downstream		7°25'N	1°26'E	150

This study was carried out using the R software (non-commercial version of S-plus). The data used in this study are the daily raw natural flows measured in m³.s⁻¹ over the period from 1991 to 2019, which show that the trend of this series varies very little and appears mainly consisted of seasonal variations. The curves represent the annual daily contributions. Yearly flows are from 1 July to 30 June of the following year and the contribution to Nangbeto Station has a cyclical evolution of 12 months. Figure 1 shows the evolution of daily natural flow rates for the period from 1991 to 2019. Each cycle is made up of a succession of 2 phases: a flood phase that extends from July to October and a low water phase that runs from November to June of the following year. The months of June and November are transition months between these two phases and therefore the year is considered for the period from July to June of the following year...

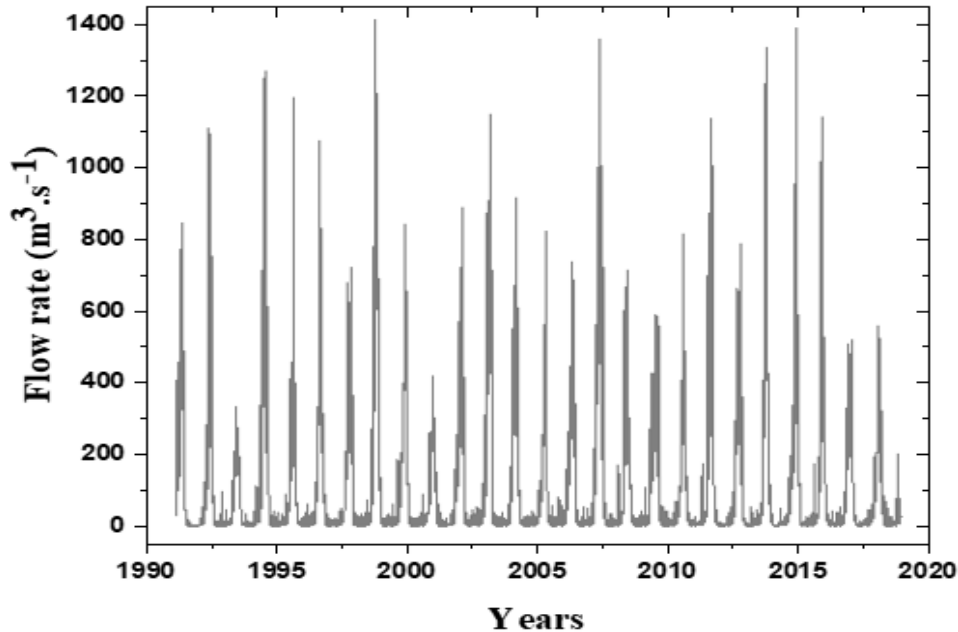


Figure 1:- Evolution of daily natural flow rates for the period from 1991 to 2019.

Methodology:-

The multiplicative deterministic model [40] was used for the modeling and forecasting of flows.

Modelling and forecasting of daily flow rates by ARIMA process

The approach proposed by Box and Jenkins (1976)[25] is applied to the flow rates series, a 28-year time series in which the frequency of observations is daily, and the periodicity was annual. This period was 365 days.

Elimination of seasonal variations of the series by standardization

This standardization is given by the following formula:

$$Z_{v,t} = (X_{v,t} - \mu_t) / \sigma_t \tag{1}$$

where $v = 1, 2, \dots, 26$; $t = 1, 2, \dots, 365$; v is the number of a year; t is the number of a day in a year; $X_{v,t}$ is the flow rate of the day t in the year number v ; and μ_t is the empirical average of the flow rates of the day number t over the 26 years of observations, that is:

$$\mu_t = \frac{1}{26} \sum_{v=1}^{26} X_{v,t} \tag{2}$$

σ_t^2 is the variance of the flow rates of the day number t over the 26 years of observations, that is:

$$\sigma_t^2 = \frac{1}{26} \sum_{v=1}^{26} (X_{v,t} - \mu_t)^2 \tag{3}$$

Modeling and forecasting of daily flow rates by the multiplicative model

The multiplicative model [24] implemented consisted in characterizing the flows from a seasonal adjustment of the series by the method of centered moving averages. This descriptive statistical model involves the calculation of probabilities and supposes that the observation of the series at time t is a function of time t and of a variable ε_t , centered in error on the model, representing the difference between the reality and the proposed model (see table 2

of the calculation of adjustment errors). The variable X_t is written in terms of error as the product of the trend by a component of the seasonality

$$X_t = C_t S_t \epsilon_t \text{ with } t = 1, 2, \dots, n \tag{4}$$

Where X_t is the series of flow rates studied, C_t is the trend component, S_t is the seasonal component and ϵ_t is the residual or random component.

Table 2:- Adjustment errors.

ARIMA model (18,1,2)	Number of days	er (%)	em (m ³ /s)	Erm
Adjustment	9490	24.74	56.87	0.27

The trend of the series of flow rates varies very little because it is almost formed of seasonal variations. Thus, in order to expunge the series of its periodic intra-annual variations or in other words, to seasonally adjust the series, we use as a mathematical technique the method of centered moving averages which has the advantage of making no prior assumptions on the form of the tendency to estimate. The order of the moving average that we use to seasonally adjust the series is 365. Indeed, the seasonality or period of this series is 365 days. The trend was estimated by regression of the seasonally adjusted series as a function of time.

$$X_t = (\alpha + \beta t) \times \left(\sum_{i=1}^{365} S_i Y_t^i \right) \times \epsilon_t ; \text{ where } Y_t^i = \begin{cases} 1, & \text{if it corresponds today} \\ 0, & \text{otherwise} \end{cases} \tag{5}$$

The process ϵ_t is then modeled by an ARIMA model ($p, d, \text{ and } q$).

Results and Discussions:-

Modeling and forecasting of daily flows by multiplicative process

The daily flow is modeled from a seasonal separation of the data series using the centered moving average method [27].

Identification of the composition scheme

The regression line of the standard deviations as a function of the mean of the flows for each year studied is provided by the following equation:

$$\sigma = 1.833t - 16.8016 \tag{6}$$

Where the coefficient 1.833 is very significant and its critical probability is $1,92 \times 10^{-14}$. This suggests the efficient adaptation of a multiplicative composition scheme for these daily flow rates. The general form of the equation for this type of model is:

$$y_t = C_t S_t \epsilon_t \tag{7}$$

Where y_t is the series of flow rates to be studied, C_t is the trend component, S_t is the seasonal component and ϵ_t is the residual or random component.

Seasonal separation of the series

The trend of the series of flow rates varies very little because it is almost formed of seasonal variations. Thus, in order to purge this series of its periodic intra-annual variations, or in other words, to seasonally adjust this series, the method of centered moving averages is used. This method has the advantage of making no prior assumptions on the form of the tendency to estimate. The order of the moving average used to seasonally adjust this data series is 365. Indeed, the seasonality or period of this series is 365 days.

Calculation of the seasonallyadjustedseries

Figure 2 presents the seasonallyadjustedseries and an estimate of the long-termoverall trend of the series of flow rates.

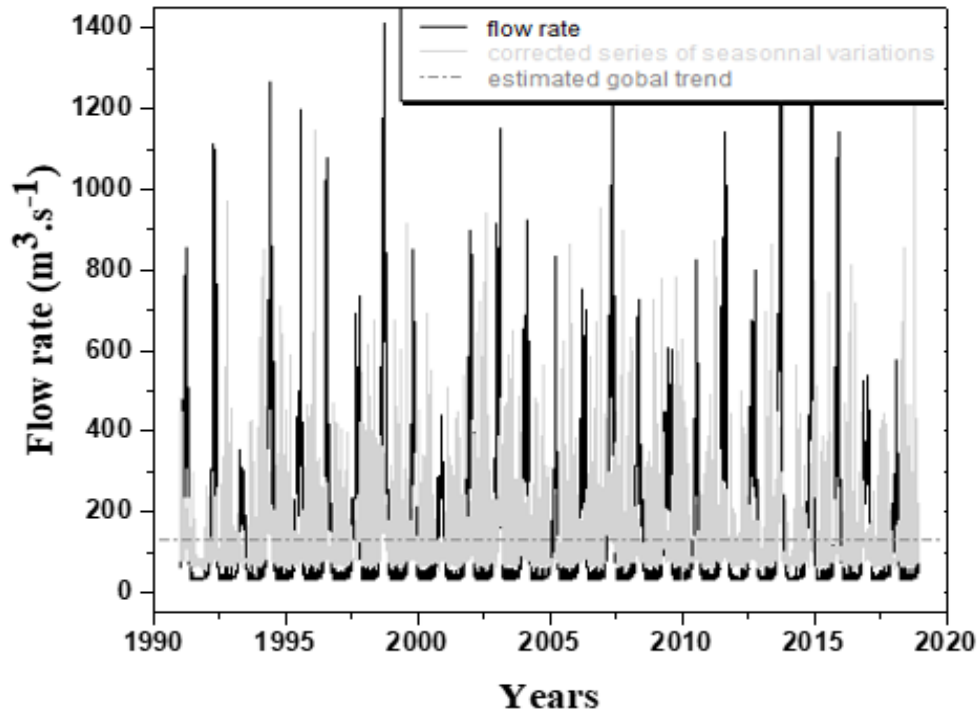


Figure 2:- Seasonallyadjustedseries.

The seasonallyadjustedserieswhichis an estimate of the overall long-term trend of the dischargeseries (Figure 2) shows thatit isalmost constant. This trend wastestimated by regression of the seasonallyadjustedseries as a function of time. The equation for thisestimated trend is:

$$C_t = 0.00667t + 106 \tag{8}$$

Where the coefficients 0.00667 and 106 have critical probabilities of 0.095 and 2×10^{-16} respectively. Thus, the slope of this line is not significant and intercept is very highly significant at the threshold of 5%. The general equation of this model is:

$$y_t = (\alpha + \beta t) \times \left(\sum_{i=1}^{365} S_i \gamma_t^i \right) \times \varepsilon_t ; \text{ where } \gamma_t^i = \begin{cases} 1, & \text{if } t \text{ correspond to day } i \\ 0, & \text{otherwise} \end{cases} \tag{9}$$

Estimation and study of residuals

Based on the precedingresults, thisestimated model has the followingform:

$$\hat{y}_t = 106 \times \left(\sum_{i=1}^{365} S_i \gamma_t^i \right) \times \varepsilon_t \tag{10}$$

Where S_i are the seasonal coefficients.

To check whether the residualsresulting from the adjustment of flows by thisestimated model form a white noise the process ε_t is studied throughitsestimated values.

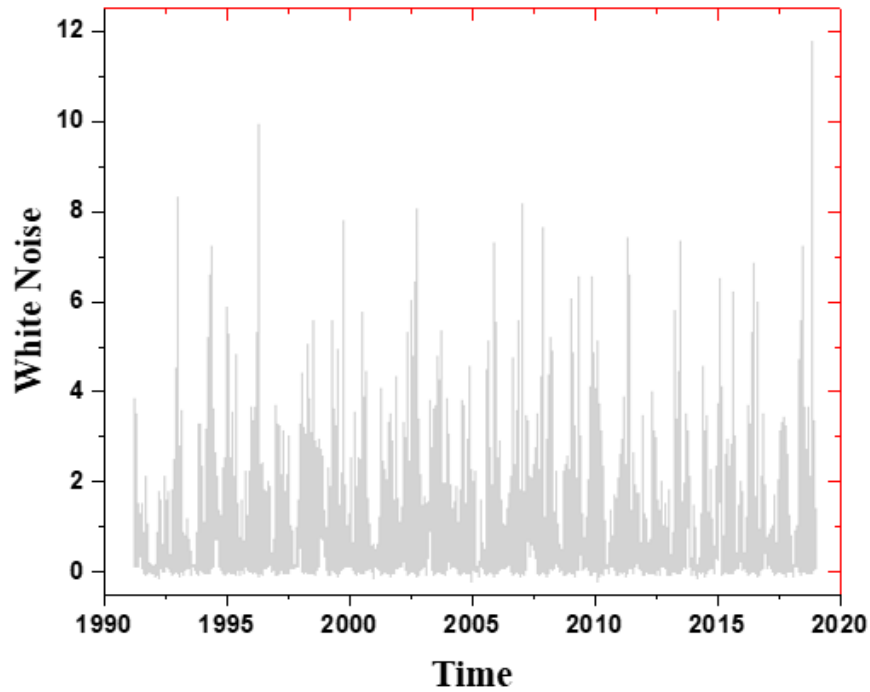


Figure 3:- Graph of standardized residuals.

Figure 3 shows the graph of the estimated residuals $\hat{\varepsilon}_t = \frac{y_t}{\hat{y}_t}$. The autocorrelation graph (Figures 4a and 4b) shows that the process $\hat{\varepsilon}_t$ is not stationary (slow decay of autocorrelations). $\hat{\varepsilon}_t$ is not white noise.

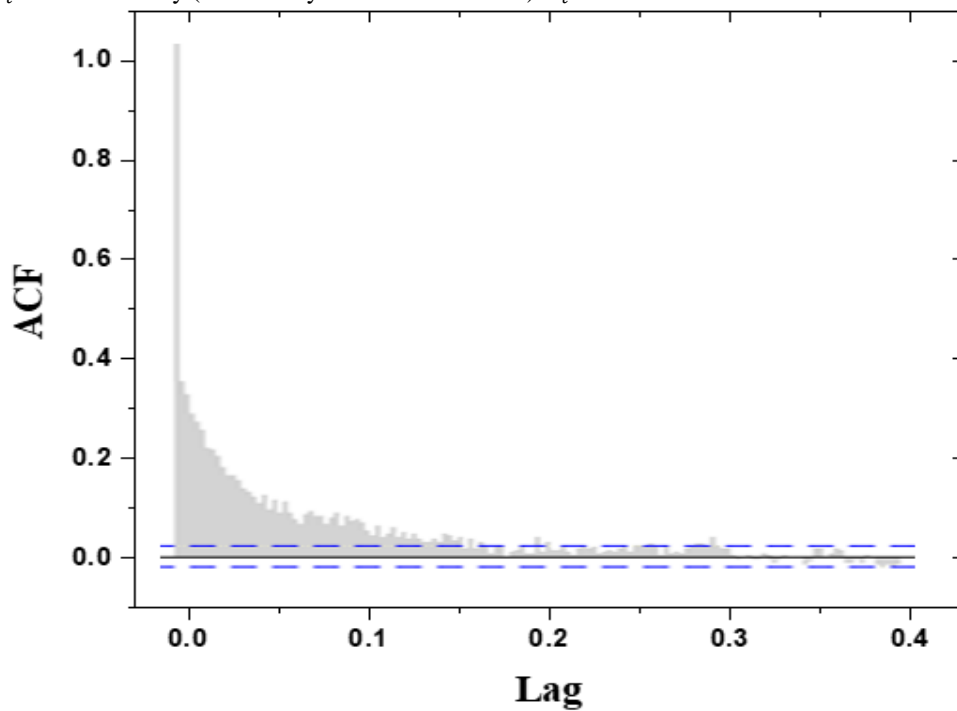


Figure 4a:- ACF of standardized residuals.

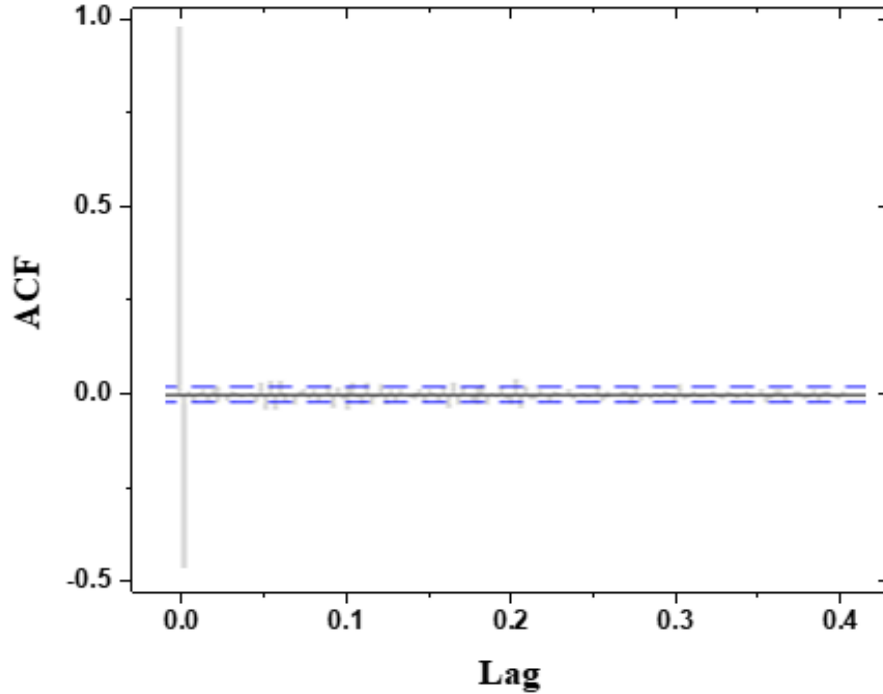


Figure 4b:- ACF of standardized and differentiated residuals.

By observing the correlogram and the partial correlogram of the process:

$$w_t = (1 - B)\epsilon_t \tag{11}$$

The process w_t appears stationary (figure 6). Then ϵ_t is modelled by an ARIMA model $(p, 1, q)$. The observation of auto-correlograms (Figure 14) enables to increase the possible pairs (p, q) by the pair $(22, 4)$. After multiple modeling with different values of the couple (p, q) satisfying this condition, we maintained the pair $(20, 3)$ as the one for which the model's AIC is minimal. The ARIMA model $(20, 1, 3)$ verified by the ϵ_t the process has the general equation:

$$\sum_{i=1}^{20} (1 - ar_i B^i)(1 - B)\epsilon_t = (1 + ma_1 B + ma_2 B^2 + ma_3 B^3) \eta_t \tag{12}$$

Where η_t is a white noise of variance, the estimated parameters of this model as well as the corresponding confidence intervals recorded in Table 3 show that the coefficients ar_{20} and ma_3 are significant. By verifying the hypothesis of the white noise of the residues η_t of this model, we observe that these residuals form indeed a white noise (Figure 14).

Table 3:- Coefficients of the multiplicative model.

ARIMA model (18,1,3)	2,5%	coef	97,5%	ARIMA model (18,1,3)	2,5%	coef	97,5%	ARIMA model (18,1,3)	2,5%
ar1	-0.0521	0.1421	0.3364	0.0991	ar12	0.0163	0.0094	0.0352	0.0131
ar2	0.5645	0.7656	0.9667	0.1026	ar13	0.0171	0.0087	0.0345	0.0132
ar3	-0.0544	0.0142	0.0259	0.0205	ar14	0.0423	0.0165	0.0093	0.0132
ar4	-0.0614	0.0263	0.0087	0.0179	ar15	0.0293	0.0035	0.0222	0.0131
ar5	-0.0394	0.0098	0.0198	0.0151	ar16	0.0248	0.0008	0.0263	0.0130
ar6	-0.0440	0.0165	0.0111	0.0141	ar17	0.0276	-0.002	0.0236	0.013
ar7	-0.0251	0.0014	0.0279	0.0135	ar18	0.0017	0.0272	0.0528	0.0130

ar8	-0.0054	0.0206	0.0466	0.0133	ar19	0.0401	0.0149	0.0104	0.0129
ar9	0.0077	0.0339	0.0602	0.0134	ar20	0.0153	0.0092	0.0337	0.0125
ar10	-0.0279	0.0009	0.0261	0.0138	am1	1.1646	0.9706	-0.7766	0.0990
ar11	-0.0505	0.0237	0.0031	0.0137	am2	0.9696	0.6473	0.3250	0.1644

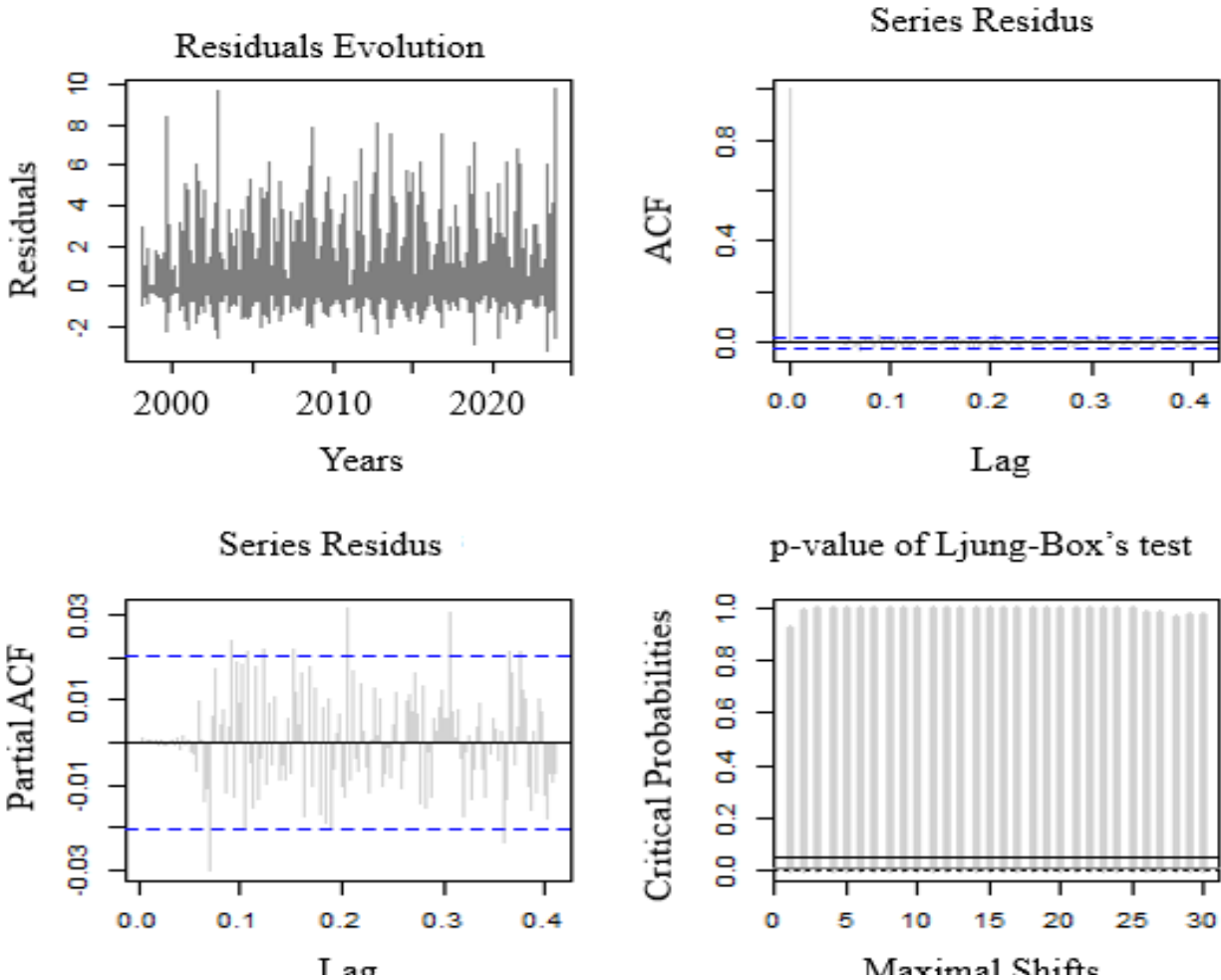


Figure 6:- Analysis of residuals of the ARIMA model(20, 1, 3).

Summary of this modeling

In sum, the equation of the model verified by the daily natural flow rates y_t is:

$$y_t = (\alpha + \beta t) \times \left(\sum_{i=1}^{365} \gamma_i S_t^i \right) \times \varepsilon_t \tag{13}$$

Where ε_t is a process that follows the ARIMA model (20, 1, 3) whose parameters are recorded in Table 2. This equation is used as the following expression to estimate the values of the series of these flow rates:

$$\hat{y}_t = \hat{\alpha} \times \left(\sum_{i=1}^{365} \hat{S}_i \gamma^i \right) \times \hat{\varepsilon}_t \tag{14}$$

where the $\hat{\varepsilon}_t$ are the process values estimated by the ARIMA model (20, 1, 3). (Figure 7) shows the adjustment of this final model with the series of actual flow rates.

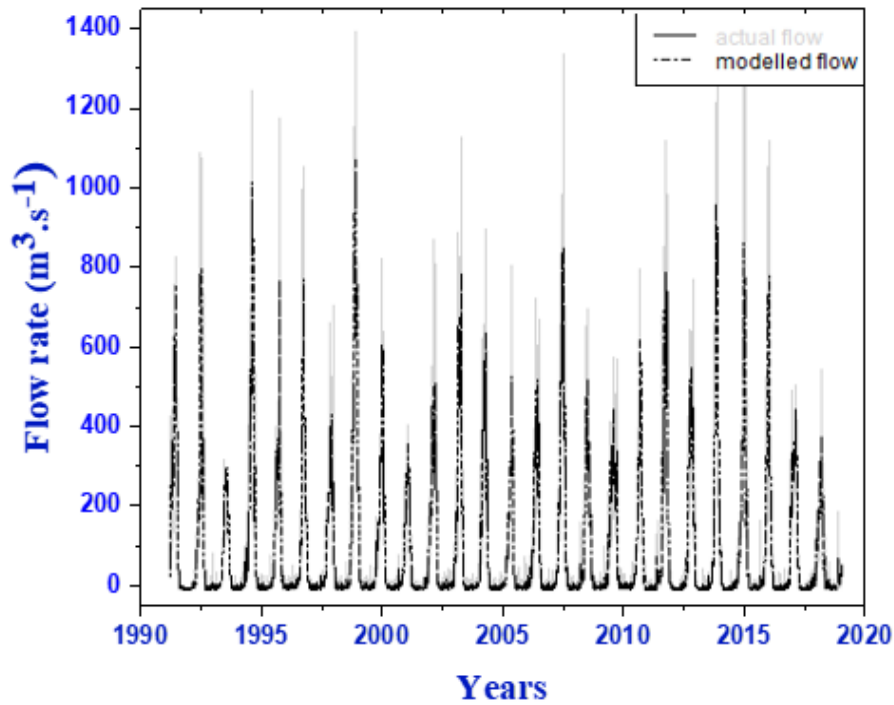


Figure 7:- Evolution of actual flow rates and adjusted flows rates by the multiplicative model.

Table 4 presents the quadratic errors related to this adjustment.

Table 4:- Quadratic errors related to this adjustment.

	Number of days	Er(%)	em(m ³ /s)	ermoy
Adjustment	9490	28.26	63.40	0.34

The following formula provides the forecast of daily natural flow rates for a fixed year k , denoted by \hat{y}_t :

$$\hat{y}_t = \hat{\alpha} \times \left(\sum_{i=1}^{365} \hat{S}_i \gamma_t^i \right) \times \hat{\epsilon}_t \tag{15}$$

Post-evaluation of the reliability of the model

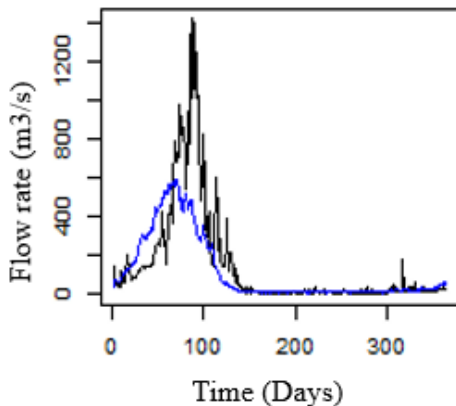
Table 5 depicts the errors of the adjustments and post predictions of the multiplicative model.

Table 5:- Errors of the adjustments and post predictions of the multiplicative model.

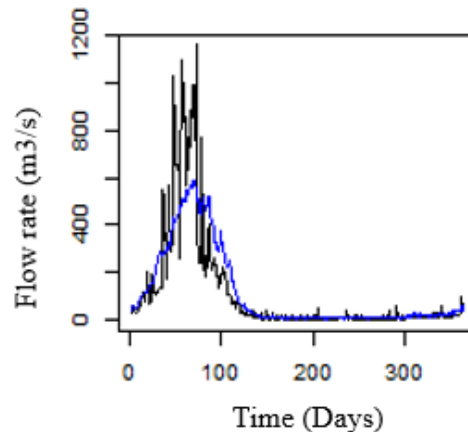
Year	Adjustment				Prediction			
	Number of days	er (%)	em (m3/s)	Emoy (m3/s)	Number of days	er (%)	em (m3/s)	emoy (m3/s)
2016	8395	28.09	63.42	0.62	365	39.02	68.31	24.14
2017	8760	28.33	63.40	0.60	365	36.87	96.45	2.9
2018	9125	27.91	63.93	0.57	365	23.16	49.62	-1.27
2019	9490	27.86	62.69	0.553	365	35.98	74.35	-3.40
2020								

Each graph in (figure 8) presents the curve of the actual flow rates on which is superimposed the one predicted by the multiplicative model.

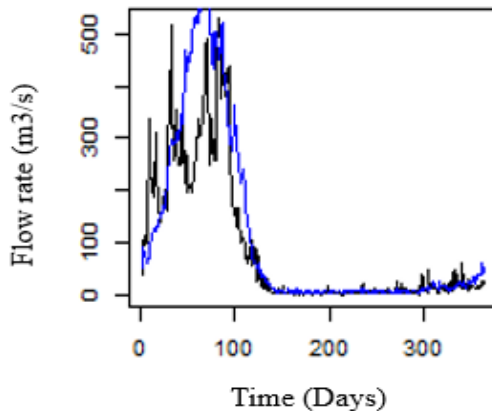
2016-2017



2017-2018



2018-2019



2019-2020

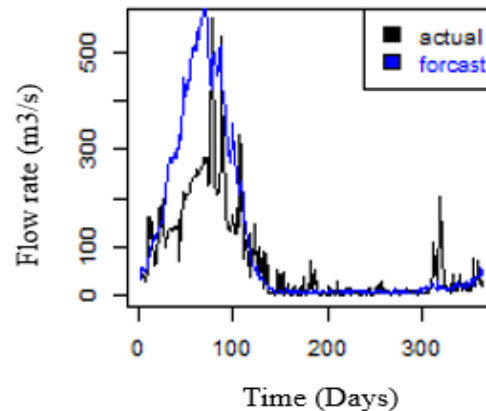


Figure 8:- Curve of actual flow rates predicted flow rates by the multiplicative model.

Conclusion:-

The determination of the flow prediction model at the Nangbeto station is carried out from the series of flows recorded from 1991 to 2019 (28 years of monitoring data). The deterministic model of the multiplicative type is suitable for the prediction of time series, after seasonal separation of the data by the method of centered mean. At the end of this research, the prediction model obtained is considered satisfactory. However, an analysis of the quadratic and relative errors shows that they are somewhat high. A program was then drawn up on the basis of the ARIMA model and it will allow water retention managers to make annual forecasts. These forecasts will be used for rational management of water retention through better planning of discharges.

References:-

1. Unduche, F., et al., (2018): Evaluation of four hydrological models for operational flood forecasting in a Canadian Prairie watershed. 63(8): p. 1133-1149.
2. Dehghani, M., B. Saghafian, and M.J.H.R. Zargar (2019): Probabilistic hydrological drought index forecasting based on meteorological drought index using Archimedean copulas. 50(5): p. 1230-1250.
3. Beyca, O.F., et al., (2019): Using machine learning tools for forecasting natural gas consumption in the province of Istanbul. 80: p. 937-949.
4. Worou, C.N., et al., (2021): Euler's Numerical Method for Ions Rejection Reassessment of a Defect-Free Synthesized Nanofiltration Membrane with Ultrathin Titania Film as the Selective Layer. Coatings, 11(2): p. 184.
5. Wanders, N., et al., (2019): Development and evaluation of a pan-European multimodel seasonal hydrological forecasting system. 20(1): p. 99-115.

6. Bugaets, A., et al., (2018): The integrated system of hydrological forecasting in the Ussuri River basin based on the ECOMAG model. 8(1): p. 5.
7. Ali, M., et al., (2020): Emergy based sustainability evaluation of a hydroelectric dam proposal in South Asia. 264: p. 121-496.
8. Kouadio, K.C.A., et al., (2020): Analysis of hydrological dynamics and hydropower generation in a West African anthropized watershed in a context of climate change. 6(4): p. 2197-2214.
9. Biswas, A.K.J.E.d., (1992): Aswan dam revisited. p. 67-69.
10. Abdelmoneim, H., et al., (2021): Inferring the Joint Operation of High Aswan Dam and Toshka Lakes using Multi-Sensor Satellite Approach. Copernicus Meetings.
11. Mulat, A.G., S.A.J.J.o.W.R. (2014): Moges, and Protection, Assessment of the impact of the Grand Ethiopian Renaissance Dam on the performance of the High Aswan Dam.
12. Adje, K., et al., (2021): Etat de la contamination en éléments traces des sédiments du Lac du barrage hydroélectrique de Nangbéto (Togo).
13. Fagbémi, M.N.A., et al., (2021): Genetic structure of wild and farmed Nile tilapia (*Oreochromis niloticus*) populations in Benin based on genome wide SNP technology. 535: p. 736432.
14. Laïbi, R., et al., (2012): Apport des séries d'images LANDSAT dans l'étude de la dynamique spatio-temporelle de l'embouchure de l'estuaire des fleuves Mono et Couffo au Bénin, avant et après la construction du barrage de Nangbéto sur le Mono. 10(4): p. 179-198.
15. Ndour, A., et al., (2018): Management strategies for coastal erosion problems in West Africa: analysis, issues, and constraints drawn from the examples of Senegal and Benin. 156: p. 92-106.
16. et après la construction du barrage de Nangbéto sur le Mono. 10(4): p. 179-198.
17. Ndour, A., et al., (2018): Management strategies for coastal erosion problems in West Africa: analysis, issues, and constraints drawn from the examples of Senegal and Benin. 156: p. 92-106.
18. Zwahlen, R., (2003): Identification, assessment, and mitigation of environmental impacts of dam projects, in *Modern Trends in Applied Aquatic Ecology*. Springer. p. 281-370.
19. Amoussou, E., et al., (2020): Climate and extreme rainfall events in the Mono River basin (West Africa): investigating future changes with regional climate models. 12(3): p. 833.
20. Xu, G., et al., (2020): A dam deformation prediction model based on ARIMA-LSTM. in 2020 IEEE Sixth International Conference on Big Data Computing Service and Applications (BigDataService). IEEE.
21. Lederoun, D., et al., (2016): Length-weight and length-length relationships and condition factors of 30 actinopterygian fish from the Mono basin (Benin and Togo, West Africa). 40(4): p. 267-274.
22. Amoussou, E., et al., (2017): Hydroclimatic variability and flood risk on Naglanou and Akissa forests areas in Mono River Delta (West Africa). 9(6): p. 212-223.
23. Amoussou, E., et al., (2018): Sedimentary evolution and ecosystem change in Ahémé lake, south-west Benin. 377: p. 91-96.
24. HOUNAHO, S.G.-F. (2020): Socio-economic and climate change effects on Fishing Yields and Farming in the Mono River Basin: Case Study of Toho Lake. PAUWES.
25. Gottwald, G.A., I.J.P.o.t.R.S.A.M. Melbourne (2013): Physical, and E. Sciences, Homogenization for deterministic maps and multiplicative noise. 469(2156): p. 20130201.
26. Tseng, F.-M., G.-H.J.F.S. Tzeng, and Systems (2002): A fuzzy seasonal ARIMA model for forecasting. 126(3): p. 367-376.
27. Fard, A.K., M.-R.J.J.o.E. Akbari-Zadeh, and T.A. Intelligence (2014): A hybrid method based on wavelet, ANN and ARIMA model for short-term load forecasting. 26(2): p. 167-182.
28. Grande, J.A., et al., (2010): Quantification of heavy metals from AMD discharged into a public water supply dam in the Iberian Pyrite Belt (SW Spain) using centered moving average. 212(1): p. 299-307.